Article

The Fundamental Principles and Standard Evaluation for Fluid Loss and Possible Extensions of Test Methodology to Assess Consequences for Formation Damage

Karl Ronny Klungtvedt [1,2,*], **Arild Saasen** [2], **Jan Kristian Vasshus** [1], **Vegard Bror Trodal** [2], **Swapan Kumar Mandal** [1], **Bjørn Berglind** [1] and **Mahmoud Khalifeh** [2]

1   European Mud Company AS, 4033 Stavanger, Norway; jkv@emcas.no (J.K.V.); sm@emcas.no (S.K.M.); bb@emcas.no (B.B.)
2   Department of Energy and Petroleum Engineering, University of Stavanger, 4021 Stavanger, Norway; arild.saasen@uis.no (A.S.); vegardtrodal@gmail.com (V.B.T.); mahmoud.khalifeh@uis.no (M.K.)
*   Correspondence: krk@emcas.no

Abstract: Industry testing procedures such as ANSI/API 13B-1 describe a method for measuring fluid loss and studying filter-cake formation against a medium of either a filter paper or a porous disc, without giving information about potential formation damage. Considering the thickness of the discs, it may also be possible to extend the method to gain an insight into aspects of formation damage. A new experimental set-up and methodology was created to evaluate changes to the porous discs after HTHP testing to generate insight into signs of formation damage, such as changes in disc mass and permeability. Such measurements were enabled by placing the disc in a cell, which allowed for reverse flow of fluid to lift off the filter-cake. Experiments were conducted with different drilling fluid compositions to evaluate the use of the new methodology. The first test series showed consistent changes in disc mass as a function of the additives applied into the fluid. The data yield insights into how the discs are sealed and to which degree solids, fibers or polymers are entering the discs. A second series of tests were set up to extend the procedure to also measure changes in the disc's permeability to air and water. The results showed that there was a positive correlation between changes in disc mass and changes in permeability. The conclusions are that the methodology may enable identifying signs of formation damage and that further studies should be conducted to optimize the method.

Keywords: fluid loss; formation damage; lost circulation; drilling fluids; filter-cake removal

1. Introduction

Different types of lost circulation materials (LCMs) are available for preventative or reactive treatment of fluid loss using procedures such as ANSI/API 13B-1 [1]. Categorization of such materials has been conducted; however, due to different application methods and different design criteria, no consistent evaluation method has been established [2]. For sealing of larger fractures, testing using slotted discs are often used and maximum sealing pressures measured. Jeennakorn et al., 2017 and 2018 [3,4] showed that varying testing conditions might give different results when testing lost circulation materials. Variations in drilling fluid compositions such as using different base fluids, density, and weighting materials impact LCM performance. Additionally, it was shown that different time-dependent degradation could occur under severe downhole conditions.

In 2018, Alshubbar et al. [5] studied the performance of LCM under conditions of an annular flow of fluid. By varying the circulation rates, they found that higher circulation rates led to higher fluid losses before a seal could be established. In addition, they identified that LCM with lower specific gravity was less prone to variations in the circulating conditions making them better preventative approach candidates.

Alsaba et al., 2014 [6] concluded that fibrous materials showed the best performance among conventional LCM in terms of sealing fractures in tapered discs and in maintaining the integrity of the formed seal within the fractures. They obtained sealing pressures up to 20.2 MPa (2925 psi) before failure when sealing a disc with a 1.0 mm fracture tip. Further, they concluded that the superior performance of the fibrous materials was considered to be due to the wide range of particle sizes and the irregularity in particle shapes and degree of deformability. In contrast, they concluded that granular materials such as $CaCO_3$ and graphite formed seals with relatively low integrity. In 2019, Khalifeh et al. [7] conducted high-pressure slot testing of fiber-based LCM demonstrating sealing performance where the seal did not fail even with pressures of more than 34.5 MPa (5000 psi) being applied. Further, it was shown that seals were dynamically built to withstand higher differential pressure.

Saasen et al., 2018 [8] tested lost circulation materials using a coarse gravel bed in addition to testing on slotted discs with the objective of testing materials for healing severe losses of drilling fluid to the formation. They found that addition of short fibers reduced filtration in porous formations and that use of long fibers may heal severe losses in fractured formations. Lee et al., 2020 [9] conducted parametric studies in numerical simulations to better understand thermal effects of sealing mechanisms of lost circulation materials. By studying properties such as fluid viscosity, particle size, friction coefficient, and Young's modulus they found that thermally degraded properties lead to inefficient fracture sealing.

In 1975, Enstad [10] described how dry powders might block hoppers with openings several times larger than the size of the dry powders. However, when transferring particles in a liquid or drilling fluid, different mechanisms will interact and change the particle plugging behavior. Whitfill 2008 [11] proposed a method for selecting a particle size distribution (PSD) based on the expected fracture width, where the D50 value should be equal to the fracture width to ensure the formation of an effective seal or plug. In 2015, Alsaba et al. [12] studied lost circulation materials of different shapes and their ability to seal fractures up to 2000 μm. They concluded that PSD had a significant effect on the seal integrities, and in particular the D90 value. It was found that a D90 value, which was equal or slightly larger than the fracture width, was required to initiate a strong seal. When combined with finer particles, the permeability of the seal would be lower, and the fluid loss reduced. A study of sealing pressure prediction [13] also found that in after the fracture width and fluid density, the D90 value was the most significant influence of sealing pressure.

The observation of particle size degradation of $CaCO_3$ and graphite, primarily due to the influence of shear, was also observed by Hoxha et al., 2016 [14]. In their studies the D50 values of medium grade $CaCO_3$ decreased by 25–40% after 30 min of shearing. Further, it was found that various methods for measuring the PSD yielded different results. As an example, the change in D50 value of regular grade graphite was recorded to be reduced between 20% to circa 70%.

In 1999, Pitoni et al. [15] studied how changes in solids composition of reservoir drilling fluids impacted forming of filter-cakes and return permeabilities. They found that filter-cake became softer and thickness increased with increasing solids content in the fluid. However, they observed that the higher the clay content, the thinner and harder the filter-cake. Additionally, the fluids with higher clay contents gave a lower return permeability. They also concluded that the size of the bridging particles effectively could be increased for high permeability or poorly consolidated formations, by adding coarse bridging particles and running the system in a "sacrificial" manner.

When conducting core flood studies to assist in designing of drilling and completion fluids in 2017, Green et al. [16] found that the lowest permeability alterations did not correlate with the lowest drilling fluid filtrate loss volumes. They concluded that the major formation damage is more likely to be caused by the drilling fluid filter cake's ability to stick to the formation and whether it can be removed during production.

Czuprat et al., 2019 [17] conducted experiments with long-term (14 days) static aging of drilling fluids and testing of fluid properties including filtration behavior and formation damage tests on sandstone samples and reservoir rock. They concluded that lower solids content in the drilling fluid would result in a slower build-up of the filter-cake, thus allowing for a higher amount of fluid filtrate invasion to occur. Additionally, they concluded that the long test period might be impractical for a service company to conduct tests before selecting a drilling fluid.

When drilling a reservoir formation with a water-based drilling fluid, polymers are used to provide viscosity and to control filtration losses. Khan et al. [18] showed that polymers such as xanthan gum, long-chain poly anionic cellulose (PAC) and starch may help in reducing fluid losses to the formation. If the pore-throats are exceeding, e.g., 20 µm and differential pressures exceeding 3.45 MPa (500 psi), such polymer additives may have little effect in preventing solids from entering the formation. PAC with shorter chains and lower viscosity (PAC LV) impact are used to reduce fluid losses through their bonding to solids in the drilling fluid and to pore-throats in the formation.

Cobianco et al., 2001 [19] developed a drill-in fluid for low permeability reservoirs using a fluid consisting of biopolymers, highly crosslinked starch and microfibrous cellulose. The used Portland limestone cores with permeability of ca. 20–100 mD for static filtration tests at differential pressures ranging from 1 to 3 MPa (145–435 psi) at 80 °C and backflowed with a 3% KCl brine to measure permeability to brine. They found that when the drilling fluid including cuttings, the return permeability was slightly lower than the formulation without the cuttings. SEM micrographs indicated that cuttings invasion was limited to the first 100 µm.

Nelson 2009 [20] conducted a study on pore-throat sizes in siliciclastic rocks and found that they form a continuum from the submillimeter to the nanometer scale. He found that reservoir sandstones generally have pore sizes greater than 20 µm and pore-throat sizes greater than 2 µm. The data reported by Nelson are hence consistent with also using discs with a median pore-throat size of 20 µm to represent a sandstone formation.

Reservoir formation damage may take place through different mechanisms [21]. It is a generic term that refers to impairment of the permeability of petroleum-bearing formations by various adverse processes. The impairment may take the form of a mechanical mechanism, such as, e.g., fines migration, solids invasion or phase trapping, or in the form of biological mechanisms or chemical mechanisms.

The literature shows that test procedures (e.g., types of fluids, applied pressure and temperature, type of flooded medium, type and geometry of LCM, etc.) create inconsistency in results obtained by different researchers. Some research study changes in formation damage by measuring changes in permeability to a fluid using rock cores. These cores are of a different nature than the discs used for the day-to-day testing of fluid loss, as per ANSI/API13B-1, thereby making such testing less accessible for a researcher or a fluid engineer.

Therefore, in this article, experiments were set up to understand the data set that is typically collected when conducting HTHP test according to ANSI/API13B-1. Thereafter, new testing methods are investigated to identify if new information about fluid loss and formation damage could be collected by extending the test procedures and using the same permeable discs. The overall objective is to use such methods for further product development and evaluation or optimization of drilling fluids. If cost-effective test methods can be established, it will facilitate more effective research and more consistent comparison of various drilling fluid compositions. The objective of the research was to identify a cost-effective method for testing drilling fluids and drilling fluid additives and to verify if this method could be used to provide reliable information about formation damage or indication of formation damage. The introduction of a moisture analyzer to precisely measure the mass change of the discs may be such a cost-effective method for identifying formation damage.

2. Analytical Approach

An experimental setup was therefore built with the following main objectives and functionalities:

- Enabling reverse flow of a fluid through the discs, after the HTHP tests, to understand filter-cake lift-off pressures.
- Enabling measurement of disc mass before and after the HTHP test and filter-cake removal to obtain indications of polymer or solids invasion into the discs.
- Enabling disc permeability estimation before and after the HTHP test and filter-cake removal to obtain indications of changes in disc permeability.
- Studying fluid loss profiles and filter-cake building.
- Establishing a practical routine for application of breaker fluid or acid to remove filter-cake.
- Understanding how various fluid degradation methods may impact the fluid loss and reservoir formation damage.

In order to investigate these potential changes in methodology, the two different base fluids shown in Appendix A, Tables A1 and A5 with KCl, xanthan gum and PAC were used. The effect of incorporation of different solids particles in the form of bentonite, $CaCO_3$, micronized barite and three types of cellulose-based fibers was investigated. The objective of using different base fluids and different fibers was to verify if the methodology could be valid for different types of fluid compositions. As the verification on the methodology was the primary objective of the research, the actual product names are not used in the descriptions. Experiments were set up with discs of mean pore-throats of 20 μm, 120 μm and 250 μm to reflect different permeability formations.

2.1. Key Factors in Fluid Loss Measurement Using Water-Based Drilling Fluids

Field engineers evaluate the properties of drilling fluid during operations to understand the requirement for potential treatment of the fluid to obtain certain desired parameters. One of these tests will normally be an HTHP test to understand filter-cake properties and the drilling fluid's ability to create a temporary seal against permeable formation.

2.1.1. Equipment for Testing According to ANSI/API 13B-1

In addition to conventional laboratory equipment for mixing (e.g., hot-rolling drilling fluids, pH and rheology measurements), the primary equipment required is an HTHP cell, which allows for testing on filter paper and permeable discs. In the experiments that were conducted, the following equipment was used:

- Hamilton Beach Mixer, Virginia, USA;
- Ohaus Pioneer Precision PX3202, New Jersey, USA;
- Ofite Filter Press HTHP 175 mL, Double Capped, Texas, USA;
- Ofite Viscometer model 900, Texas, USA;
- Ofite roller-oven #172-00-1-C, Texas, USA;
- Apera pH90, pH meter, Wuppertal, Germany.

2.1.2. Test Procedure and Data Collection in Accordance with ANSI/API 13B-1

For the full procedure, please refer to the ANSI/API 13B-1 for water-based drilling fluids or ANSI/API 13B-2 for oil-based drilling fluids [22]. The information contained herein contains only the main elements. The filtration tests are conducted at high temperature and high pressure under static conditions using a pressurized gas source to create a differential pressure across the test medium. The test medium used is either a filter paper, typically with a median pore-throat of 2.5 μm or permeable ceramic discs with means pore throats ranging from 10 to 250 μm. After the differential pressure has been applied and the temperature in the cell has reached the desired level, the cylinder outlet valve is opened to enable the differential pressure to drive the fluid towards the medium. The fluid filtrate

is thereafter collected and measured over a 30-min period. For comparison with other tests, one needs to account for differences in filter area. The data collected according to the procedure is:

- Measure the filter-cake thickness, at its center, to the nearest millimeter (or 1/32 in).
- Observe indications of settling of solids on the filter-cake, such as an abnormally thick cake or coarse texture, and record comments.
- The filtrate volume V_f should be measured and normalized with regards to filter area.

2.2. Extending the HTHP Filtration Tests to Study Signs of Formation Damage

The objective is to collect information related to formation damage and other operational parameters and to identify if the methodology can yield meaningful information about potential formation damage.

2.2.1. Equipment Overview

The experimental set-up was centered around a cell with regulated supply of pressured air to drive a fluid or air through the ceramic discs. The experiments were not planned for filter paper, as the filter paper is not designed for higher pressures than 3.45 MPa (500 psi). By reversing the discs into the cell, fluid can be pumped through the disc at low pressures to study the lift-off pressure of filter-cakes, as shown in Figure 1. Further, by measuring both the supply pressure and flowrate, estimates of disc permeability could be conducted. Extending the procedure further, a moisture analyzer was used to measure the mass of the disc in a standardized dry condition before the HTHP test and after the test including reverse flow and any breaker application. The following equipment was used for the experimental set-up in addition to the standard equipment used for the HTHP test according to ANSI/API 13B-1:

- Ohaus MB120 Moisture Analyzer;
- Custom built transparent acrylic cell with stand for enabling of reverse flow of fluid through the ceramic discs;
- Festo pressure regulator LRP-1/4-2.5 and LRP-1/4-0.25;
- Festo Pressure Sensor SPAN-P025R and SPAN-P10R;
- Festo Flowmeter SFAH-10U;
- Nitrogen source and manifold for pressure up to 9.3 MPa (1350 psi), Ofite #171-24;
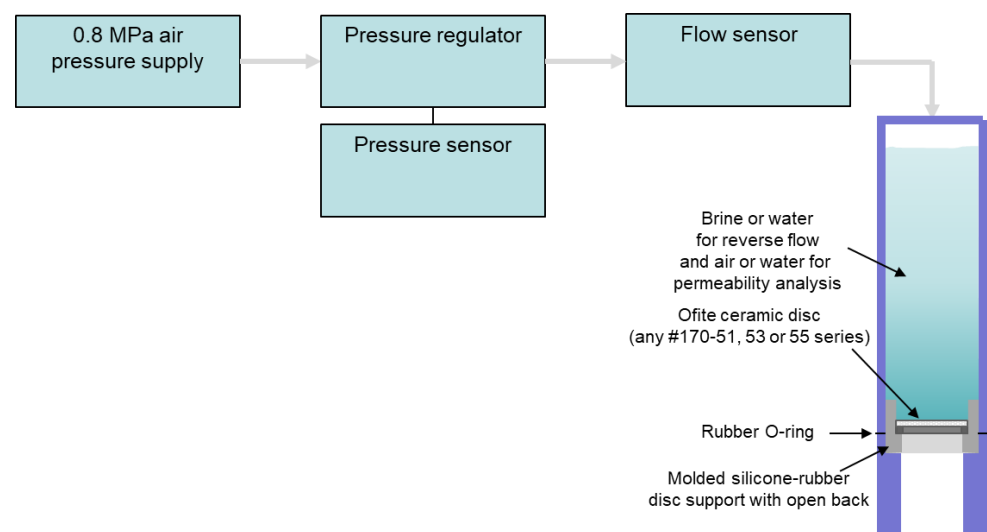- Vacuum machine, DVP EC.20-1.

Figure 1. Infographic of the system developed for this study.

2.2.2. Procedures Applied for Testing Using Experimental Set-Up

The main elements of the new procedure are the measurement of disc mass and permeability to water and air before and after the HTHP test. For the full procedure and calculations, please refer to Appendix B. Testing of permeability was restricted to discs with mean pore-throat size of 20 μm as it was difficult to establish precise readings of pressure and flow rate with flow of air or water through the higher permeability discs. A permeability analysis of other disc grades may be practical with a higher viscosity fluid. Otherwise, the procedure was the same for all ceramic disc grades.

3. Experimental Data

3.1. Identifying Signs of Polymer, Solids or Fiber Invasion into Permeable Formations Using a Moisture Analyzer to Measure Changes in Disc Mass

In total, 11 different samples were tested according to the procedure described in Appendix B, including 16 h of hot-rolling at 90 °C, six of which were tested on ceramic discs with a specified median pore-throat size of 120 μm (Ofite #170-53-4) and five of which were tested on 250 μm discs (Ofite #170-53-6). All tests were conducted at 6.9 MPa (1000 psi) differential pressure and 90 °C. An overview of the tests is shown in Table 1. Fiber A and Fiber B were selected from two different manufacturers of cellulose-based lost circulation materials, based on relatively similar specified particle size distributions.

Table 1. Test overview for high-permeability discs.

Test Number	Description of Test
1	Base fluid (with bentonite and $CaCO_3$), normal mixing, 120 μm disc
2	Base fluid, high-shear mixing, 120 μm disc
3	Base fluid, high-shear mixing, 250 μm disc
4	Base fluid plus FIBER A, normal mixing, 120 μm disc
5	Base fluid plus FIBER A, high-shear mixing, 120 μm disc
6	Base fluid plus FIBER A, normal mixing, 250 μm disc
7	Base fluid plus FIBER A, high-shear mixing, 250 μm disc
8	Base fluid plus FIBER B, normal mixing, 120 μm disc
9	Base fluid plus FIBER B, high-shear mixing, 120 μm disc
10	Base fluid plus FIBER B, normal mixing, 250 μm disc
11	Base fluid plus FIBER B, high-shear mixing, 250 μm disc

Five of the tests were conducted after a 30-min high-shear mixing procedure to identify any particle degradation. The same degradation test was conducted separately for some of the wet-sieving tests referenced in Figure 2. The degradation tests indicated that $CaCO_3$ degraded partially during the high-shear mixing procedure. Initially, the wet sieving showed 15.7% and 15.8% of particles being larger than 90 μm, equivalent to a concentration of 13.4–13.5 kg/m^3 in the respective fluid samples. After the high-shear mixing, the concentrations of particles larger than 90 μm was reduced to 9.7% and 9.2%, respectively, implying that circa 40% of the particles above 90 μm had been degraded, and that the resulting concentrations in the fluid samples would be 8.3 kg/m^3 and 7.9 kg/m^3. In contrast, the high-shear mixing of FIBER A did not show signs of degrading, and the concentration was kept stable around 10.6 kg/m^3. One test, which included bentonite, showed an increase in concentrations of FIBER A above 90 μm after high-shear mixing. Since the high-shear mixing of FIBER A without bentonite did not show the same effect, it was considered that a potential cause of the apparent increase in the concentration of larger particles may be bentonite particles piggybacking on the coarser FIBER A particles

to increase the measured concentration of such particles. Tables A2 and A3 in Appendix A gives more detailed information about dry sieving and wet sieving results.

Particle concentration >90μm
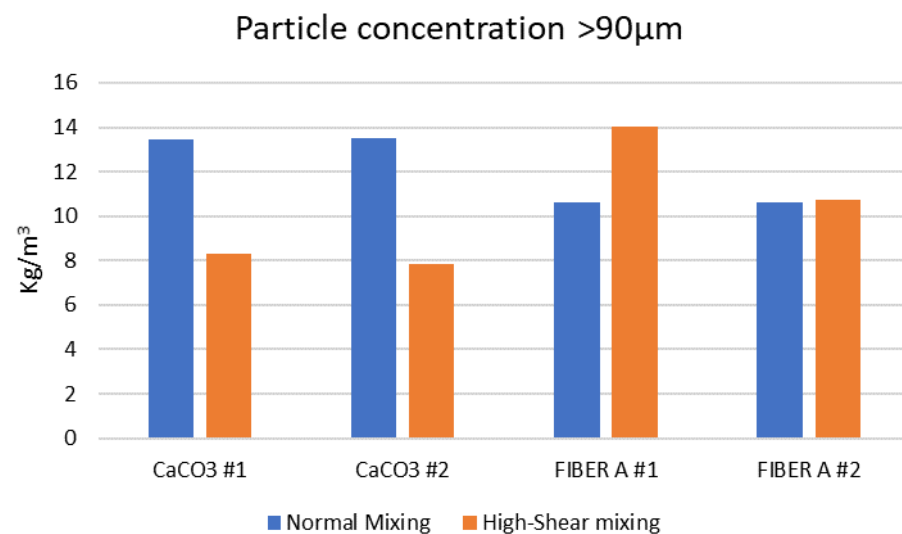
Figure 2. Changes in particle concentration in fluid due to high-shear degradation.

Figure 3 shows the HTHP tests on the 120 μm discs on the left, with each of the three mixtures of (i) the base fluid being KCl-Polymer drilling fluid with CaCO3, (ii) the base fluid plus FIBER A, and (iii) the base fluid plus FIBER B. The tests were conducted with and without high-shear degradation. The fluid loss tests showed that the base fluid produced a fluid loss of 31 mL before degradation and that the fluid loss increased to 42 mL after degradation. The fluid with FIBER A showed a fluid loss of 31 mL before degradation, but unlike the base fluid, the sealing efficiency increased after the high-shear degradation and gave a fluid loss of 25 mL. The fluid with FIBER B also showed an improvement after the degradation test, where the fluid loss was 45 mL without degradation and just over 31 mL after degradation.

The fluid loss profiles were generally consistent throughout the testing on the 120 μm discs. After the initial spurt-loss, the loss-rates were gradually falling during the test and appeared to approach a linear curve with a fluid loss rate of around 0.2 mL/min after 20 min. The development of the fluid loss may indicate that the filter-cake had substantially been formed within the first 15 s, but that further thickness was built over time and that a more stable permeability achieved after 10–20 min.

The testing on 250 μm discs, shown in the right half of Figure 3, was planned to be identical to the testing on the 120 μm disc, however, the base fluid with $CaCO_3$ recorded a total loss during the first few seconds of the test, so no further tests were conducted with the base fluid alone. The testing of the two fiber-based products FIBER A and FIBER B showed considerably improved results relative to the testing on the 120 μm ceramic. Contrary to expectations, the fluid losses recorded on the 250 μm discs were significantly smaller than on the 120 μm disc, and the fluid loss rates were showing a different profile. Again, the tests showed lower fluid losses after the high-shear degradation tests. The main difference, however, was the observation of more erratic fluid losses during the 30-min test. It was several times observed that the fluid loss appeared to stop, and then restarted again at more irregular intervals.
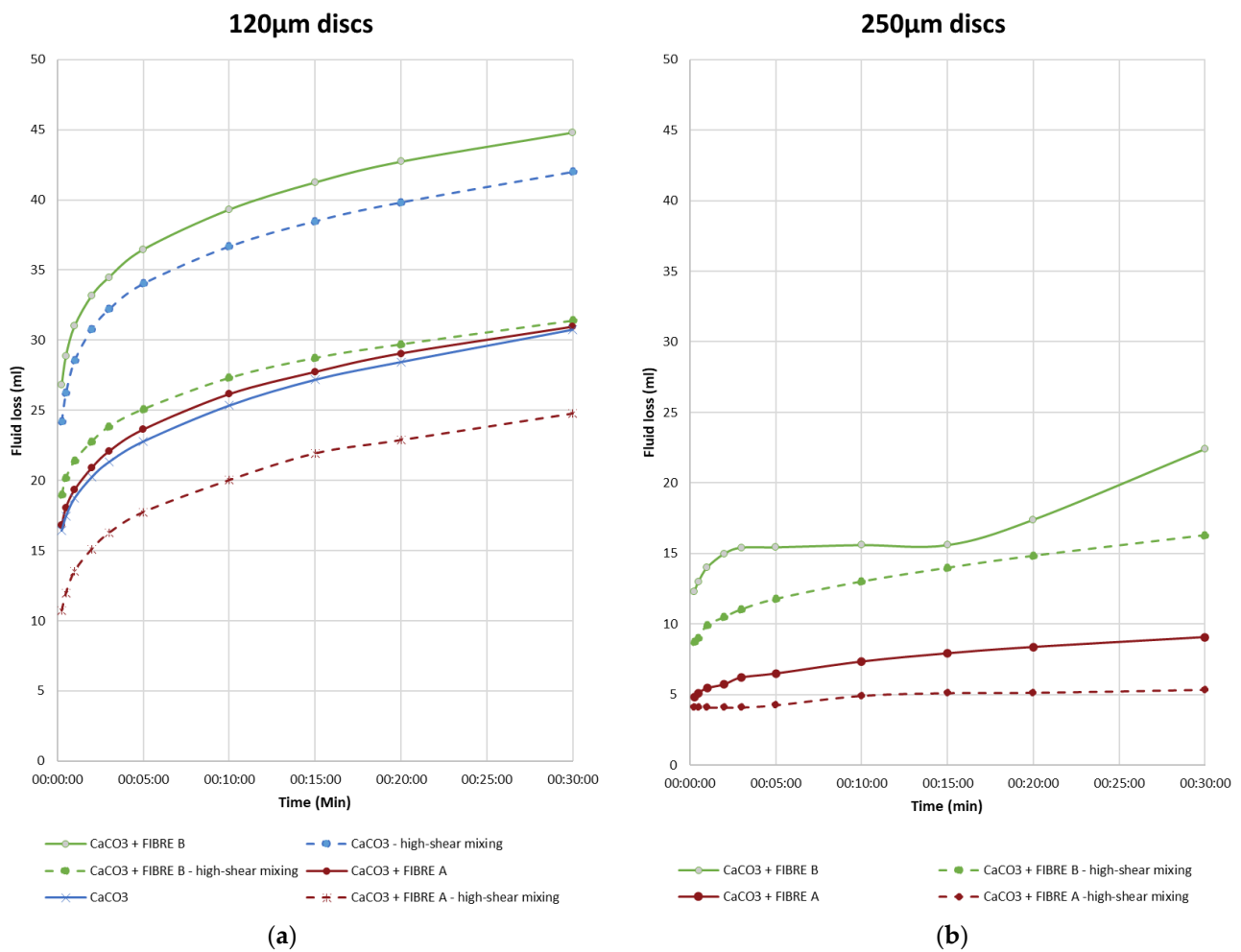
Figure 3. Fluid loss on high-permeability discs, (**a**) 120 µm discs and (**b**) 250 µm discs.

By comparing the filter-cakes from the different tests, it was clear that the building of the filter-cakes followed a different mechanism on the coarser discs. The filter-cakes formed on the 120 µm discs were of a uniform nature and thicker than the more irregular filter-cakes on the 250 µm discs, as seen in Figure 4. The impression was that the combined particles of the $CaCO_3$ and the fibers created a layered mat on the surface of the 120 µm disc, whereas the single or collections of particles were plugging larger pores on the 250 µm discs.

When conducting the low-pressure reverse flow of brine through the discs (<7 psi or <0.05 MPa), the filter-cakes were easily removed from the 120 µm discs as the filter-cakes came off either whole or in large pieces. Little visual trace of the filter-cakes was left on the disc other than along the circumference, which was held back by the silicone mold, which held the disc inside the acrylic cell, see Figure 5 as an example.
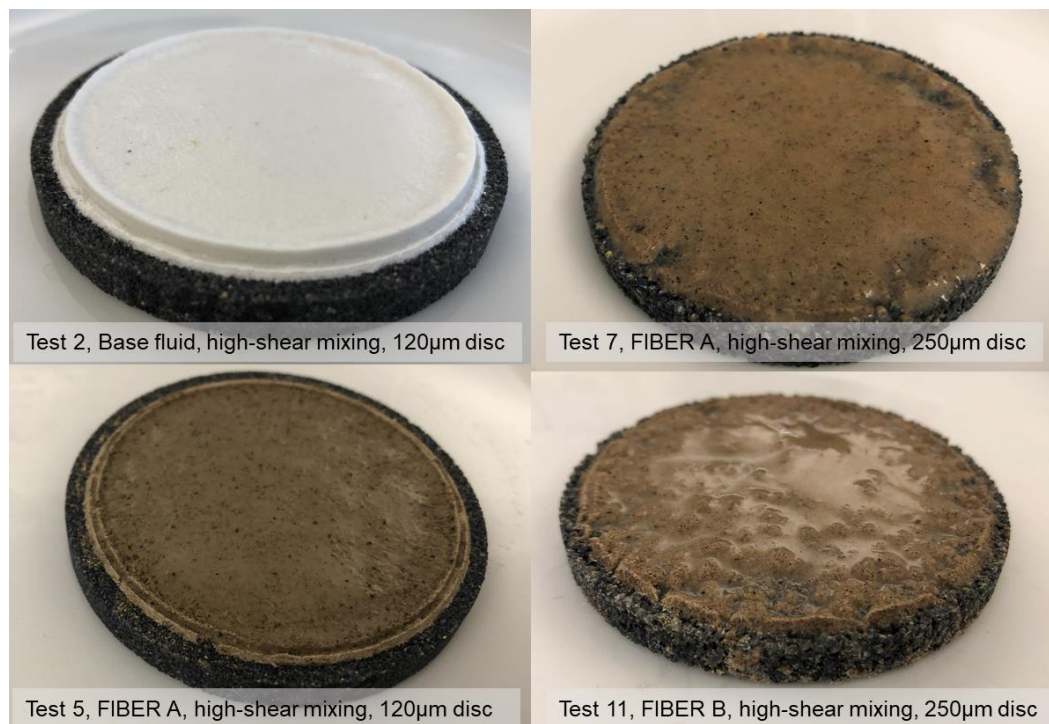
Figure 4. Filter-cakes after the 6.9 MPa (1000 psi) HTHP fluid loss test.
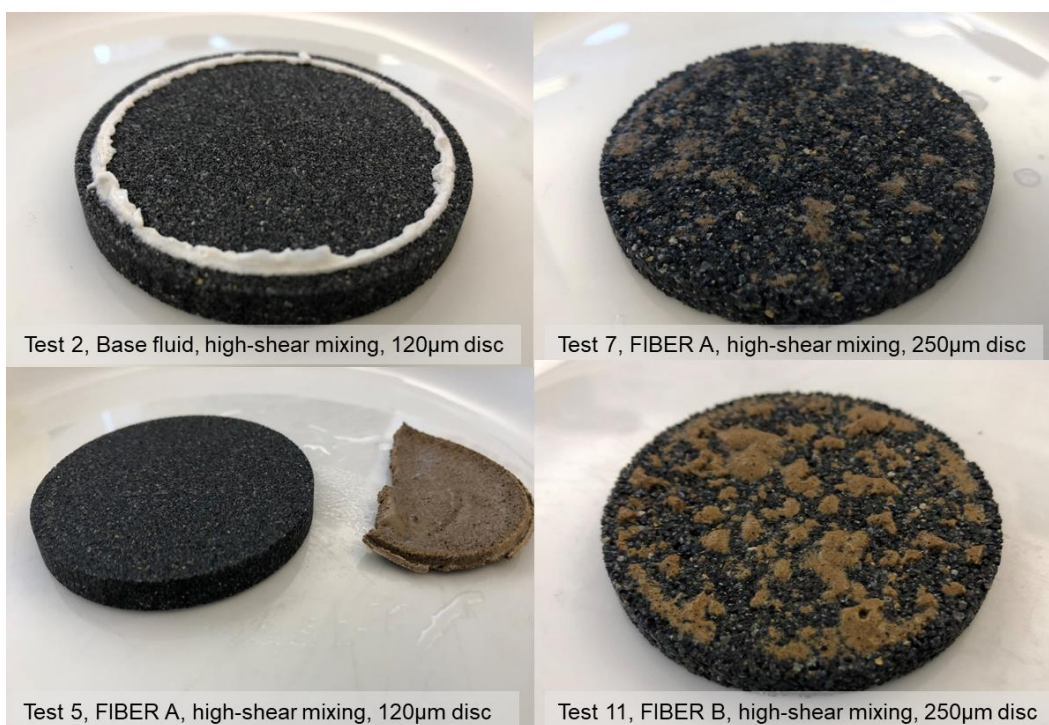
Figure 5. Discs after reverse flow with brine at 0.05 MPa pressure.

On the 250 μm discs, the filter-cakes were noticeably more separated as they were washed off the discs. This may be due to the filter-cake being thinner than for the 120 μm discs. Visual inspection showed minor particles protruding from the surface of the discs, giving further substance to the impression of particles partly penetrating and plugging the pore-throats of the discs.

Following the reverse flow, the discs were placed in a liquid oxidizing breaker and kept at a temperature of 90–100 °C for four hours. The discs were thereafter flowed with water to remove any loose residue and dried in the moisture analyzer. The discs were visually inspected for traces of residue and the final disc masses compared with the original disc masses to identify any invasion of polymer, solids or fiber. Figure 6 shows the discs from testing of FIBER A after removal of filter-cakes. By visual inspection no particle or filter-cake residue could be identified. In contrast, some residue could be seen into the pore-throats of the 250 µm discs in Figure 7, after testing of FIBER B, thereby the indicating particle-plugging inside the disc.
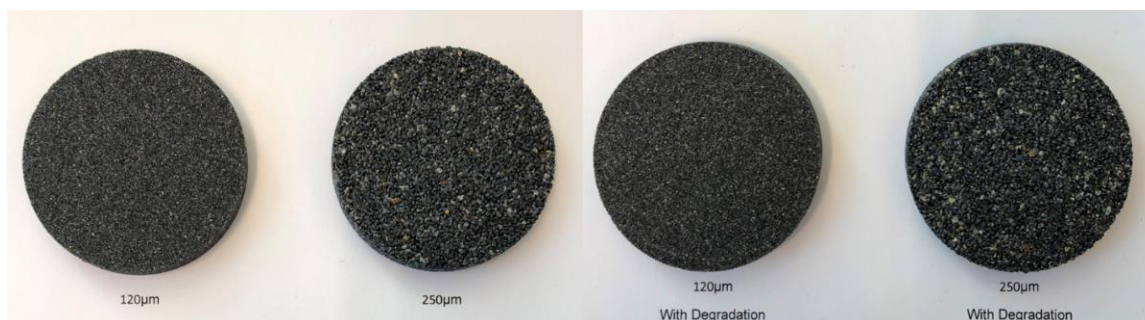
Figure 6. Discs for testing of FIBER A after breaker application.
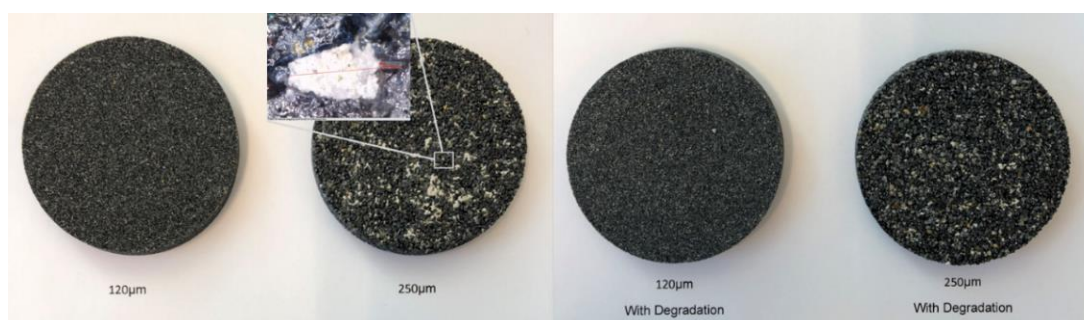

Figure 7. Discs for testing of FIBER B after breaker application.

By placing both the fluid loss measurements and disc mass gain data into one chart, some interesting observations can be made, see Figure 8.

Tests 1 and 2 with the base fluid including $CaCO_3$ show that nearly all of the filter-cake and potential invasion of polymers and solids into the discs have been removed by the reverse flow and breaker application. In contrast, test number 3 recorded a total loss of fluid and no pressure control. This corresponded with a more significant increase in disc mass, which may be due to residue of polymers and solids. This clearly indicates that formation damage may occur when the particles are of insufficient size to create a low-permeability filter-cake.

The four tests conducted with FIBER A show an inverse relationship between increase in disc mass and fluid loss. After visual inspection of the filter-cakes, it looked like the filter-cakes on the 250 µm showed more of a particle-plugging nature, whereas the filter-cakes on the 120 µm discs to a greater extent were created uniformly and externally to the disc. The measurements of increase in disc mass were consistent with this theory, as low increases in disc mass were recorded on the 120 µm discs, and more significant increases in disc mass was recorded on the 250 µm discs, where particle plugging, or deep sealing was suspected.
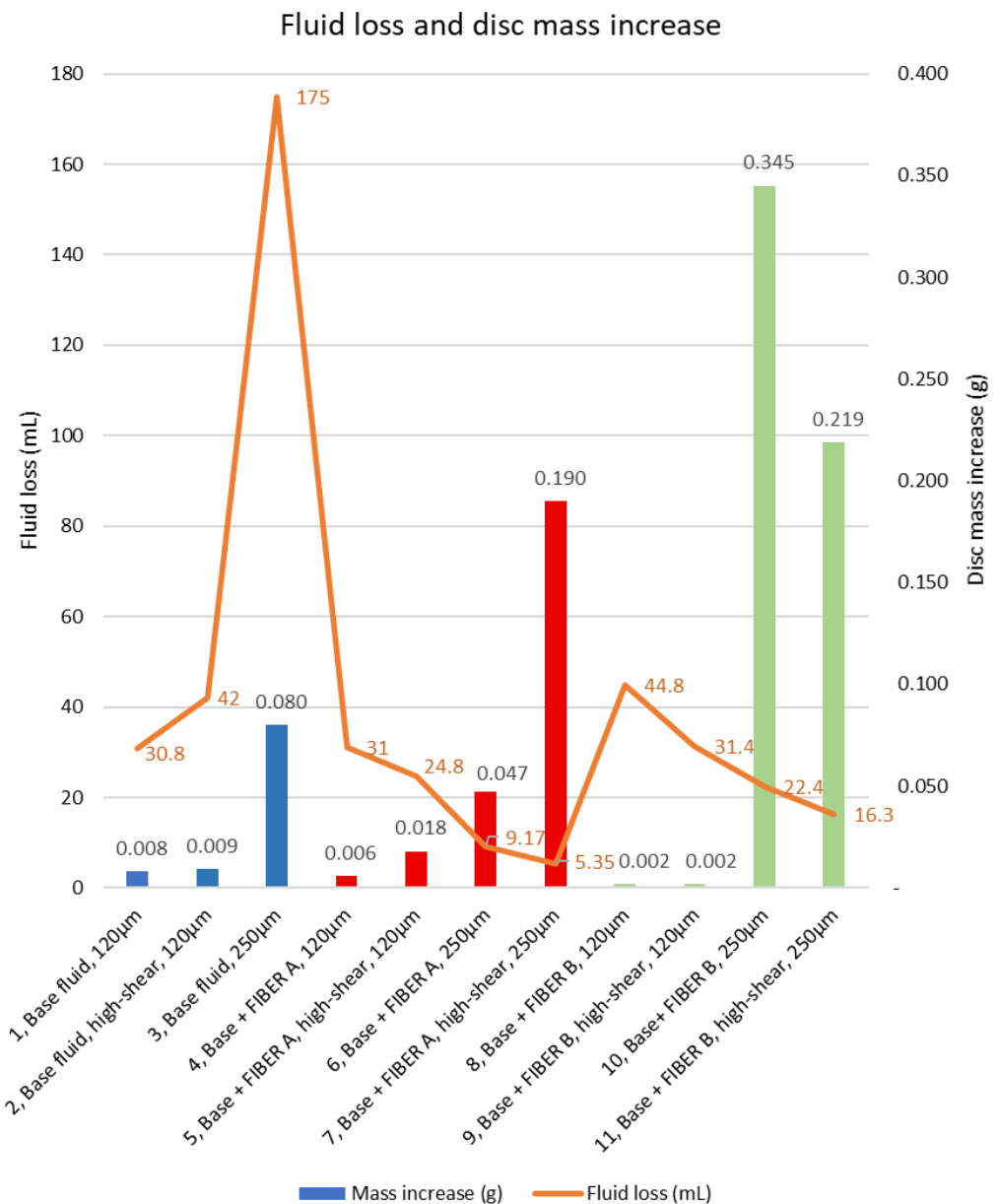
Figure 8. Fluid loss and disc mass increase.

The tests with FIBER B were consistent with the observations from the testing of FIBER A. Disc mass increases were negligible on the finer discs, whereas the mass increases of the coarser discs were the largest in the test. The full data for disc mass measurements can be found in Table A4 in Appendix A.

Dry-sieving tests indicated that both FIBER A and FIBER B had a weight concentration of 13–14% with particles larger than 180 µm, whereas only 1% of the $CaCO_3$ was larger than 180 µm. As such a lower sealing ability of the 250 µm discs without the presence of any of the fiber products could be expected. The sealing of the 120 µm discs was shown to be falling as the percentage of $CaCO_3$ particles was reduced after degradation in test number 2, relative to test number 1, as also shown in Figure 2. A 90 µm particle size represents 75% of the specified median pore-throat size of the 120 µm discs. This may be an indication that particles above 75% of the median pore-throat size of the disc may be required to form an effective filter-cake.

3.2. Extending the Testing Regime to Include Estimation of Disc Permeability Changes

A new set of tests was conducted to study potential changes in the permeability of ceramic discs with specified mean pore-throat size of 20 μm (Ofite #170–53-3). The tests were conducted using the full test-procedure specified in Appendix B. Four tests were conducted with a KCl-Polymer fluid with combinations of Bentonite and FIBER UF as sealing-materials, refer to Appendix A, Table A5 for the full recipe. Due to finer discs being used than in the tests referred to in Section 3.1, a finer grade fiber was selected. FIBER UF was provided by the vendor with a specified D90 of 75 μm and a D100 of 90 μm. The rheology of the various fluid compositions was measured before and after hot-rolling. The measurements showed slight increases in shear stress for a given shear rate as more particles were added to the fluid, as shown in Figure A1, Appendix A.

The disc grade was chosen such that it would be practical to test water-permeability and air-permeability, in addition to the changes in disc mass as described in Section 3.1. Discs with median pore-throat size larger than 20 μm were found to be more difficult to test, as the flowrates of fluid would be very high relative to the low pressures applied. Table 2 show the main data from tests 12–15. As an initial experiment, it was chosen to use water to test permeability even though this would not represent a reservoir fluid. The objective was only to ascertain if the method had practical value, rather than to be an exact replication of a reservoir drilling situation in presence of hydrocarbons.

Table 2. Fluid loss and formation damage data for tests 12–15.

Test	Fluid Loss	Disc Mass Change	Water Permeability Retention	Air Permeability Retention
12, Base fluid 2	Total loss	From 42.031 to 42.279 g = +0.248 g	From 3.338 to 0.997 D = 30%	From 2.327 to 0.822 D = 35%
13, Base fluid 2 + 14.3 kg/m^3 (5 ppb) FIBER UF	24.2 mL	From 41.394 to 41.419 g = +0.025 g	From 4.056 to 2.253 D = 56%	From 2.824 to 2.378 D = 89%
14 Base fluid 2 + 28.5 kg/m^3 (10 ppb) Bentonite	32.2 mL	From 40.776 to 40.795 g = +0.029 g	From 5.633 to 3.166 D = 56%	From 2.823 to 2.686 = 95%
15, Base fluid 2 + 28.5 kg/m^3 (10 ppb) Bentonite and 14.3 kg/m^3 (5 ppb) FIBER UF	19.8 mL	From 40.990 to 40.986 g = −0.004 g	From 5.329 to 3.459 D = 65%	From 3.479 to 3.037 D = 87%

The fluid loss data showed that the Base Fluid 2 (test 12) could not withstand the 6.9 MPa (1000 psi) pressure and build a filter-cake. The HTHP fluid loss test was therefore aborted after around 2–3 s. The reverse-flow of brine through the disc at 0.075 MPa (11 psi) showed very little fluid flow. The disc mass measurement showed that the test with the Base Fluid 2 created a significant increase in the disc mass of 248 mg. Due to the fluid not containing either solids or fiber, the disc mass increase was likely reflecting polymer damage to the formation. The measurements of permeability to water indicated that only 30% of initial permeability had been retained during the test. A thin layer of residue was visible on the surface of the disc where the filter-cake should have been formed.

Test 13 showed that the addition 14.3 kg/m^3 (5 ppb) of FIBER UF could seal the disc without the presence of solids and produced a fluid loss of 24.2 mL. The reverse-flow of brine through the disc at 0.075 MPa (11 psi) showed very moderate fluid flow, but the filter-cake did not lift off directly. After application of breaker, the filter-cake was dissolved and the measurement of permeability to water showed that 56% of original permeability had been retained. The disc mass measurement showed a low increase of mass of 25 mg. Only a slight change in color on the surface showed that there had been a filter-cake on the disc prior to the application of the breaker fluid.

By adding 28.5 kg/m^3 (10 ppb) of bentonite instead of the fiber, test 14 was completed with a fluid loss of 32.2 mL. Reverser flow of brine lifted off the filter-cake and fluid flow appeared relatively similar to test 13. After application of the breaker, the filter-cake was dissolved and the measurement of permeability to water showed that 56% of the original permeability had been retained. The disc mass measurement showed a low increase of

mass of 29 mg. Some light gray residue was visible on the surface of the disc after reverse flow and breaker fluid application.

The lowest fluid loss was recorded when both 14.3 kg/m^3 (5 ppb) of FIBER UF and 28.5 kg/m^3 (10 ppb) of bentonite was added to the base fluid. For this test, the fluid loss was reduced to 19.8 mL. There was no visible residue on the disc surface and the mass measurement indicated a very minor fall in disc mass of 4 mg. The measurement of permeability to water showed retention of 65%.

The information on changes in disc mass, permeability to water and air were gathered in attempt to find practical method for studying indicators of any formation damage caused by the drilling fluid in a real-life application. A differential pressure of 6.9 MPa (1000 psi) was considered to be adequately reflecting what might be experienced in certain drilling situations. Similarly, it was of interest to see if a relatively low reverse pressure of 0.075 MPa (11 psi) could start the process of filter-cake removal before any chemical cleaning of the reservoir was applied.

It was shown that the addition of either FIBER UF or bentonite reduced the invasion of drilling fluid into the formation and also that less damage appeared to have been made to the formation permeability. Further, the combination of FIBER UF and bentonite showed even lower fluid loss and the visual inspection and the mass measurement indicated that no or little damage to the formation had been caused. In contrast, the estimation of permeability to water showed that some change in permeability might have occurred. In this context one should consider the polarity of water and its potential interaction with bentonite and the cellulose based FIBER UF.

When studying the results of the tests it should be considered that only the first 6.35 mm ($^1/_4$″) or of the formation has been studied. The content of the fluid filtrate has not been studied, and hence it may be difficult to provide clear evidence for which further damage could have been caused to formation further away from the wellbore. During tests 13–15, the applied pressure of 6.9 MPa (1000 psi) was successfully held, and a moderate amount of fluid filtrate was collected. This may be an indication that such fluid compositions would be quite effective in preventing fluid loss to the formation. Test 12 showed that polymers alone could not seal the disc under the applied differential pressure nor prevented polymers from migrating into the disc. Figure 9 shows the discs after breaker application and drying.

Figure 9. Discs from tests 12–15 after breaker application and drying.

4. Observations and Lessons Learned from the Experimental Procedure

Measurement of disc mass using the moisture analyzer, weighing the fluid filtrate continuously during the HTHP process and calculation of fluid filtrate were practical exercises that yielded consistent results without complications.

The process of reverse flow using brine and water for lifting of filter-cake functioned very well within certain limitations. For tests where the applied differential pressure during the HTHP test was 6.9 MPa (1000 psi), certain fluid combinations showed little or no reverse flow with applied reverse pressure of 0.069 MPa (10 psi) and a brine temperature

of 60 °C. It was experimented with applying higher reverse pressures and higher brine temperatures whilst developing the method that was applied. Higher temperatures were avoided to avoid deforming of the acrylic cylinder, and higher pressures were avoided as some discs fractured if the reverse pressure exceeded 0.1 MPa (15 psi).

Calculating the average permeability to dry air functioned very well and yielded quite consistent and repeatable results on dry discs prior to any HTHP testing. The primary ambition was to identify changes to the calculated permeability of each individual disc. One observation was that the permeability of discs coming from different batches varied considerably, whereas discs coming from the same batch appeared to be more similar. The method has a weakness when used after an HTHP test as it is based on the disc being predried before flowing of air. Using this method, the effects of drying may impact discs with the presence of, e.g., polymers, solids, and fibers and their ability to obstruct flow of air differently. These data may therefore be imprecise relative to flow of fluids in a reservoir formation.

Adapting the permeability estimation to a fluid such as water appeared to be more complex. The primary observation was that the calculated permeability of an individual disc could vary, even when correcting for changes in viscosity due to temperature changes. The process that enabled a stabilization of the readings included to place the disc in fluid in vacuum to remove any air-bubbles from the disc and fluid before the test. This yielded considerably more consistent results, particularly on low-permeability discs. A cause of the uncertainty of measurement was thought to be capillary forces at the air–water interface, and the improvement obtained by placing the disc and fluid in vacuum strengthened this idea.

Additionally, it should be considered that the thickness of the discs (ΔL) is low relatively to the depth of a typical core sample for a return permeability test. The testing of the discs can therefore be considered to reflect the skin damage of a formation.

5. Conclusions

The inclusion of additional procedures to those described in ANSI/API 13B-1 yielded information relevant to obtaining a better understanding of fluid loss and giving an insight into how various drilling fluid compositions seal permeable formations and how they may impact future reservoir permeability. The main conclusions are as follows:

- By extending the testing procedure with (i) a moisture analyzer and (ii) reverse flow equipment and a procedure for reverse flow and breaker fluid application it was possible to measure the increases in disc mass accurately.
- Reverse flow of fluid through the disc with filter-cake enables studying the removal of filter-cake by back pressure.
- Application of an oxidizing breaker did in certain cases allow the test discs to return to almost its original state, with mass changes so low that they may be considered to be within the tolerances of the tests.
- As the discs median pore-throat size was varied relative to the particle size of the fibers and CaCO$_3$, for tests 1–11, it appeared that different mechanisms for sealing the disc and creating a filter-cake was obtained. Hereunder, when the solids or fibers were equal or marginally smaller than the pore-throat openings, fluid loss was reduced, and the sealing appeared to partial plugging of the pore-throats. In contrast, when a significant portion of the particles was larger than the mean pore-throat size, a thicker and more uniform filter-cake was building on the disc. Without the presence of fibers or when the solids were smaller than the pore-throats, no low-permeability filter-cake was formed, and disc mass increases were significant.
- In the tests on the 120–250 μm discs where either of the fiber products was present, there was an inverse relationship between fluid loss and disc mass increases. In the tests on the 20 μm discs, the fibers appeared to be larger than the pore-throats, and there was a positive relationship between lower fluid loss and lower disc mass increase.

- Testing of disc mass change and change of permeability to water and air suggested that ranking 20 μm discs in terms of lowest increase in mass and lowest calculated change to water-permeability would yield consistent results in terms of indicating formation damage. Since the other disc grades are built up in the same way as the 20 μm discs, it may be possible to obtain equivalent results with discs of other grades.
- The findings on using the new testing methodologies are indicating that valuable information concerning reservoir formation damage may be observed and estimated using a relatively simple set-up and test procedure. To further investigate this potential, it is recommended to conduct further experiments. One of the natural extensions of the methodology is to investigate using a non-polar hydrocarbon-based fluid for testing of permeability and for presoaking discs before the fluid loss test.

Author Contributions: Conceptualization, K.R.K.; methodology, K.R.K. and J.K.V.; formal analysis, K.R.K., B.B. and V.B.T.; writing—original draft preparation, K.R.K.; writing—review and editing, K.R.K., A.S., M.K. and S.K.M.; supervision, S.K.M. All authors have read and agreed to the published version of the manuscript.

Institutional Review Board Statement: Not applicable.

Informed Consent Statement: Not applicable.

Data Availability Statement: Data availability on request due to intellectual property rights of EMC.

Conflicts of Interest: The authors confirm that this article content has no conflict of interest.

Appendix A

Appendix A contains recipes and data from the tests.

Table A1. Recipe and mixing sequence of drilling fluid for tests 1–11.

Mixing Sequence	Material/Additive	Mass (g)
1	H_2O	328
2	Na_2CO_3	0.02
3	NaOH	0.25
4	Xanthan Gum	1.2
5	Poly-Anionic Cellulose, Low Viscosity	4.0
6	MgO	1.0
7	KCl	17.5
8	Bentonite	5.0
9	$CaCO_3$ (D50 of 50 μm)	30.0
10	With or without FIBER A or FIBER B at given concentration	8.0

Table A2. Dry sieving of drilling fluid additives for tests 1–11.

Additive	<90 μm	90–180 μm	>180 μm
$CaCO_3$	74.2%	24.8%	1.0%
FIBER A	56.3%	30.6%	13.1%
FIBER B	29.5%	56.5% *	13.9%

* When sieving of FIBER B it was noted that the particles had some magnetic properties. Visual inspection indicated that this might have increased amount of product collected in 90 μm sieve.

Table A3. Wet sieving of drilling fluid sample with additives before and after high-shear degradation for tests 1–11.

Wet Sieving before and after High-Shear Degradation	<90 μm	>90 μm
$CaCO_3$ Sample #1, normal mixing	84.3%	15.7%
$CaCO_3$ Sample #2, normal mixing	84.2%	15.8%
$CaCO_3$ Sample #1, 30 min high-shear mixing	90.3%	9.7%
$CaCO_3$ Sample #2, 30 min high-shear mixing	90.8%	9.2%
FIBER A Sample #3, normal mixing	53.4%	46.6%
FIBER A Sample #4, normal mixing	53.5%	46.5%
FIBER A Sample #5, 30 min high-shear mixing together with bentonite	38.6%	61.4%
FIBER A Sample #4, 30 min high-shear mixing	52.9%	47.1%

Table A4. Disc mass measurements in dry condition before and after whole test sequence for tests 1–11.

Test with Changes in Disc Mass	Original Disc Mass (g)	Final Disc Mass (g)	Mass Increase (g)
1, Base fluid (with bentonite and $CaCO_3$), normal mixing, 120 μm disc	50.098	50.106	0.008
2, Base fluid, high-shear mixing, 120 μm disc	50.069	50.078	0.009
3, Base fluid, normal mixing, 250 μm disc (TOTAL LOSS)	50.249	50.329	0.080
4, Base fluid plus FIBER A, normal mixing, 120 μm disc	50.419	50.425	0.006
5, Base fluid plus FIBER A, high-shear mixing, 120 μm disc	49.970	49.988	0.018
6, Base fluid plus FIBER A, normal mixing, 250 μm disc	50.624	50.671	0.047
7, Base fluid plus FIBER A, high-shear mixing, 250 μm disc	50.457	50.647	0.190
8, Base fluid plus FIBER B, normal mixing, 120 μm disc	49.789	49.791	0.002
9, Base fluid plus FIBER B, high-shear mixing, 120 μm disc	49.927	49.929	0.002
10, Base fluid plus FIBER B, normal mixing, 250 μm disc	50.139	50.484	0.345
11, Base fluid plus FIBER B, high-shear mixing, 250 μm disc	50.204	50.423	0.219

Table A5. Recipe and mixing sequence of base fluid 2 for tests 12–15.

Mixing Sequence	Material/Additive	Mass (g)
1	H_2O	328
2	Na_2CO_3	0.02
3	NaOH	0.25
4	Xanthan Gum	1.2
5	Poly-Anionic Cellulose, Low Viscosity	4.0
6	MgO	1.0
7	KCl	17.5
8	With or without Bentonite at given concentration	10.0
9	With or without FIBER UF at given concentration	5.0
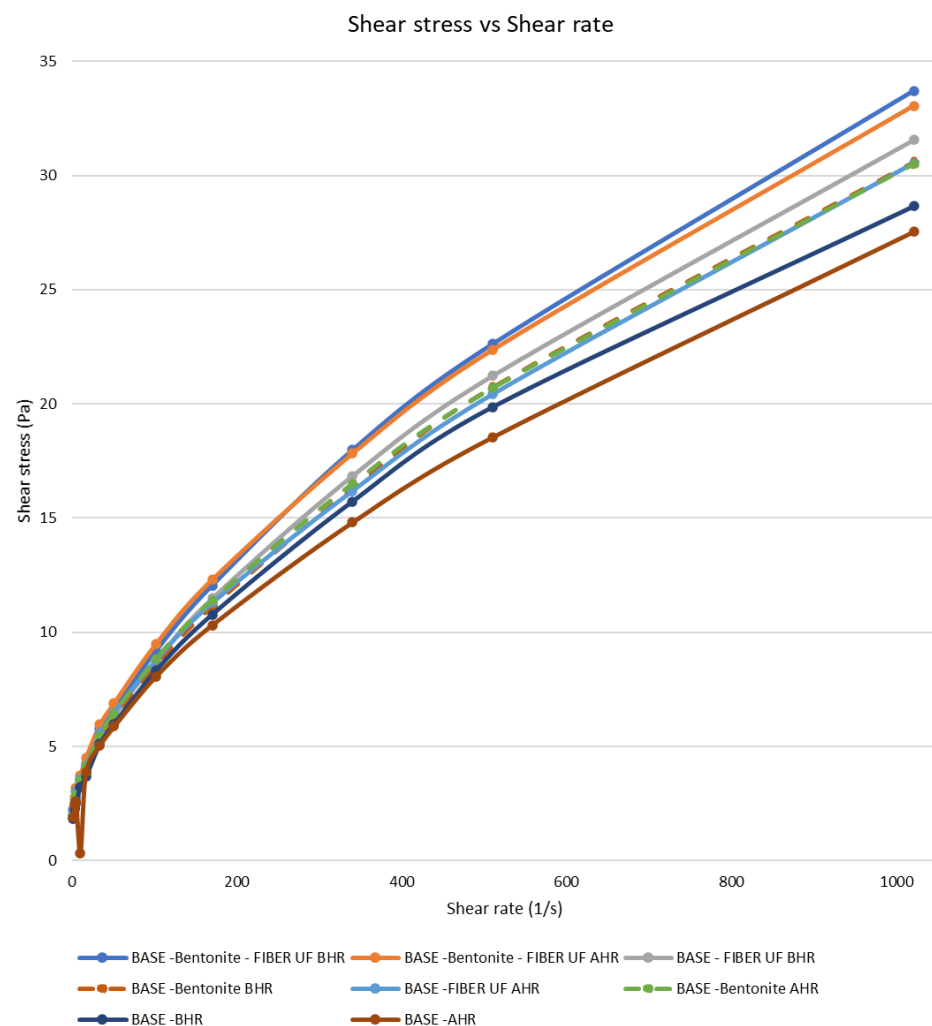
Figure A1. Rheology before hot-rolling (BHR) and after hot-rolling (AHR) of fluids for tests 12–15.

Appendix B

Procedure for measuring change in disc mass and change in permeability and relevant calculations.

1. Mix drilling fluid according to the recipe;
2. Measure pH and rheology;

3. Hot-roll and if applicable degrade by high-shear stirring or other degradation method;
4. Measure pH and rheology after hot-rolling and any degradation;
5. Mark and weigh disc in dry condition using the moisture analyzer (M_b). Moisture analyzer shall be set to dry disc at 105 °C until change in mass is less than 1 mg/60 s;
6. Optional step: place disc in acrylic cell and measure air temperature and flowrate at different pressures to calculate average permeability to air (K_{ab});
7. Optional step: place disc in acrylic cell and place arrangement with water in vacuum (circa −0.96 bar for 5 min) to remove any air from disc or water. Flow thereafter water through disc and measure water temperature and flowrate at different pressures to calculate average permeability to water (K_{wb});
8. Soak disc in brine (40 g NaCl per 1000 g freshwater) in vacuum;
9. Conduct HTHP test at desired pressure, typically 3.45 MPa (500 psi) or 6.9 MPa (1000 psi), and measure both volume (V_f) and mass (M_f) of fluid filtrate at point in time of 15 s, 30 s, 1 min, 2 min, 3 min, 5 min, 10 min, 15 min, 20 min and 30 min (V_f). Calculate fluid filtrate density;
10. Weigh disc with filter-cake and observe filter-cake;
11. Place disc in acrylic cell and reverse flow with 1 L (40 g NaCl per 1000 g water) heated to 60 °C and then with 1 L water heated to 60 °C. Note pressure required to enable reverse flow through disc;
12. Optional step: place disc in breaker fluid for required time and at required temperature. Place disc in acrylic cell and flow disc with 1 L water at ambient temperature to remove any dissolved filter-cake residue;
13. Optional step: place disc in acrylic cell and place arrangement with water in vacuum to remove any air from disc or water. Flow thereafter water through disc and measure water temperature and flowrate at different pressures to calculate average permeability to water (K_{wa});
14. Weigh disc in dry condition using moisture analyzer (M_a) using the same settings as in step 5;
15. Optional step: place disc in acrylic cell and measure air temperature and flowrate at different pressures to calculate average permeability to air (K_{aa}).

Depending on the number of optional steps included in the procedure, it enables collection of a large amount of data in addition to observing the filter-cake and the fluid filtrate volume V_f.

The moisture analyzer used for weighing the discs was set to heating the discs to 105 °C and continue drying until the mass change due to moisture evaporation was less than 1 mg per 60 s. The drying process then stopped automatically, and the mass of the disc displayed. The precision of the instrument is 1 mg. The change in disc mass was then simply calculated as:

$$(M_a) - (M_b) = M_{change}$$

By placing a digital weight under the graduated cylinder used to measure fluid filtrate, it was possible to simultaneously record the mass of the fluid filtrate and read the volume of the filtrate. This enabled a precise estimation of the fluid loss profile and calculating the fluid filtrate density (D_f), calculated as:

$$(M_f)/(V_f) = (D_f)$$

The permeability was calculated as an average of multiple readings within certain flow-rate ranges. Darcy's law was used in a rearranged form as follows:

$$K = \eta \frac{Q * \Delta L}{A * \Delta P}$$

where K is the calculated permeability coefficient (m^2), η is the viscosity of the fluid (Pa * s), Q the fluid flowrate (m^3/s), ΔL the disc thickness (m), A the areal of flow into the disc and ΔP the pressure differential over the disc (Pa).

References

1. ANSI/API 13B-1. In *Recommended Practice for Field Testing Water-based Drilling Fluids*, 5th ed.; API Publishing Sevices: Washington, DC, USA, 2019.
2. Alsaba, M.; Nygaard, R.; Hareland, G. AADE-14-FTCE-25. In *Review of Lost Circulation Materials and Treatments with an Updated Classification*; AADE: Houston, TX, USA, 2014.
3. Jeennakorn, M.; Alsaba, M.; Nygaard, R.; Saasen, A.; Nes, O.-M. The effect of testing conditions on the performance of lost circulation materials: Understandable sealing mechanism. *J. Pet. Explor. Prod. Technol.* **2018**, *9*, 823–836. [CrossRef]
4. Jeennakorn, M.; Nygaard, R.; Nes, O.-M.; Saasen, A. Testing conditions make a difference when testing LCM. *J. Nat. Gas Sci. Eng.* **2017**, *46*, 375–386. [CrossRef]
5. Alshubbar, G.; Nygaard, R.; Jeennakorn, M. The effect of wellbore circulation on building an LCM bridge at the fracture aperture. *J. Pet. Sci. Eng.* **2018**, *165*, 550–556. [CrossRef]
6. Alsaba, M.; Nygaard, R.; Saasen, A.; Nes, O.M. *Lost Circulation Materials Capability of Sealing Wide Fractures*; SPE-170285-MS; SPE International: Houston, TX, USA, 2014.
7. Khalifeh, M.; Klungtvedt, K.R.; Vasshus, J.K.; Saasen, A. *Drilling Fluids—Lost Circulation Treatment*; SPE-195609-MS; SPE Norway: Bergen, Norway, 2019.
8. Saasen, A.; Hodne, H.; Ronæs, E.; Aarskog, S.A.; Hetland, B.; Løvereide, M.B.; Mohammadi, R. *Wood Fibre Based Lost Circulation Materials*; OMAE2018-77662; ASME: Madrid, Spain, 2018.
9. Lee, L.; Taleghani, A.D. Simulating Fracture Sealing by Granular LCM Particles in Geothermal Drilling. *Energies* **2020**, *13*, 4878. [CrossRef]
10. Enstad, G. On the theory of arching in mass flow hoppers. *Chem. Eng. Sci.* **1975**, *30*, 1273–1283. [CrossRef]
11. Whitfill, D. In Proceedings of the Lost Circulation Material Selection, Particle Size Distribution and Fracture Modelling with Fracture Simulation Software, SPE-115039-MS, IADC/SPE, Jakarta, India, 25–27 August 2008.
12. Alsaba, M.; Nygaard, R.; Saasen, A.; Nes, O.M. Experimental investigation of fracture width limitations of granular los circulation materials, 2015. *J. Petrol. Explor. Prod. Technol.* **2016**, *6*, 593–603. [CrossRef]
13. Alsaba, M.; Aldushaishi, M.; Jeennakorn, M.; Nygaard, R.; Saasen, A.; Nes, O.M. *Sealing Pressure Prediction Model for Lost Circulation Treatments Based on Experimental Investigations*; AADE-17-NTCE-21; American Association of Drilling Engineers: Houston, TX, USA, 2017.
14. Hoxha, B.B.; Yang, L.; Hale, A.; van Oort, E. *Automated Particle Size Analysis using Advanced Analyzers*; AADE-16-FTCE-78; AADE: Houston, TX, USA, 2016.
15. Pitoni, E.; Ballard, D.A.; Kelly, R.M. *Changes in Solids Composition of Reservoir Drill in Fluids during Drilling and the Impact on Filter Cake Properties*; SPE 54753; SPE International: The Hauge, The Netherlands, 1999.
16. Green, J.; Patey, I.; Wright, L.; Carazza, L.; Saasen, A. *The Nature of Drilling Fluid Invasion, Clean-Up, and Retention during Reservoir Formation Drilling and Completion*; SPE-185889-MS; SPE Bergen: Bergen, Norway, 2017.
17. Czuprat, O.; Dahle, B.O.; Dehmel, U.; Ritschel, R.; Storhaug, J.; Adrian, T.; Patley, I. *Systematic Selection of Drill-in and Completion Fluids for Development of the Dvalin HT Gas Field*; SPE-195601-MS; SPE Norway: Bergen, Norway, 2019.
18. Khan, R.; Kuru, E.; Tremblay, B.; Saasen, A. Extensional Viscosity of Polymer Based Fluids as a Possible Cause of Internal Cake Formation. *Energy Sources A* **2007**, *29*, 1521–1528. [CrossRef]
19. Cobianco, S.; Bartosek, M.; Lezzi, A.; Previde, E. *New Solids-Free Drill.in Fluid for Low Permeability Reservoirs*; SPE-64979; SPE: Houston, TX, USA, 2001.
20. Nelson, P.H. Pore-throat sizes in sandstones, tight sandstones, and shales. *AAPG Bull.* **2009**, *93*, 329–340. [CrossRef]
21. Civan, F. *Reservoir Formation Damage 2020*; Gulf Professional Publishing: Waltham, MA, USA, 2020; pp. 1–6, ISBN 978-0-12-801898-9.
22. ANSI/API 13B-2. In *Recommended Practice for Field Testing Oil-Based Drilling Fluids*, 5th ed.; API Publishing Services: Washington, DC, USA, 2014.